Supplementary Materials for

Long-term pattern and magnitude of soil carbon feedback to the climate system in a warming world

J. M. Melillo,* S. D. Frey, K. M. DeAngelis, W. J. Werner, M. J. Bernard, F. P. Bowles, G. Pold, M. A. Knorr, A. S. Grandy

*Corresponding author. Email: jmelillo@mbl.edu

Published 6 October 2017, *Science* **358**, 101 (2017)
DOI: 10.1126/science.aan2874

This PDF file includes:

Materials and Methods

Detailed Site Description

Soils are of the Canton series (coarse-loamy over sandy or sandy-skeletal, mixed mesic Typic Dystrochrept), with a surface pH of 3.83 and a subsurface pH of 4.85. The average bulk density of the upper 15 cm is 0.64 g cm^{-3} (*8*). A distinct plow layer indicates past cultivation, and historical records confirm that this old-field forest was established after the abandonment of cultivation at the turn of the 20th century. There was some cutting for firewood following agricultural abandonment, but prior to initiation of our warming experiment. The climate is cool temperate and humid. At the initiation of the experiment in 1991, dominant tree species at the site were red maple (*Acer rubrum* L.) and black oak (*Quercus velutina* Lam.). During the first five full years of the experiment (1992-1996), mean weekly air temperature varied from a high of about 20ºC in July to a low of about -8ºC in February (*31*). During the five most recent years of the experiment (2012-2016), mean weekly air temperature varied from a high of about 22ºC in July to a low of about -7ºC in January (*32*). Precipitation is distributed evenly throughout the year and annually averages about 120 cm.

Detailed Warming System Description

A total of eighteen 6 x 6 m experimental plots separated by 1 m buffer zones are organized into six blocks with three plots per block (one control plot, one disturbance control plot, and one heated plot). All samples were taken from within a 5 x 5 m sampling area centered inside of each plot to minimize edge effects. Heated and disturbance control plots have heating cables (Smith-Gates Easy Heat) buried 10 cm deep, running parallel to each other, spaced 20 cm apart. When supplied with 240 V-AC, the heating cables have a power output of 13.6 W/m and produce a power density of 77 W/m^2. This method of warming has been evaluated to perform well under a variety of moisture and temperature conditions (*13*). A Campbell Scientific CR10 (1991-2011) or CR1000 (2012-present) datalogger, connected to Campbell Scientific type 107 thermistors (4 per heated plot, 1 per control or disturbance control plot), monitored soil temperature, regulated the warming manipulation of each individual plot on a 10 minute time-step, and recorded hourly soil temperatures in each experimental plot. Gaps in the temperature record were gap-filled using a model relating air temperatures recorded at a nearby eddy covariance tower (1991-2006) or the Fisher meteorological station (2007-present) to the soil

temperatures recorded in the control plots. The gap-filling model included the 4-week running mean air temperature, the 2-day running mean air temperature, an interaction term between the 4-week and 2-day running means, and year as factors. The model had an $r^2 = 0.96$ for the eddy covariance dataset and an $r^2 = 0.97$ for the Fisher dataset.

Soil Respiration Sampling and Modeling

Soil CO_2 flux rates were measured approximately monthly from April through November each year using the fixed chamber technique (*33*). Chambers, constructed of 1.8 cm thick polyvinyl chloride (PVC) plastic, consisted of a cylindrical 28.7 cm diameter - 4:0 cm tall chamber top and a 5.2 cm tall lower portion (anchor). Anchors, installed at the start of the experiment, were pushed 1-2 cm into the organic horizon to minimize disturbance and secured in place with stainless steel stakes. Litter was allowed to accumulate normally inside of the collars. Although we have not measured fine root biomass inside of the collars (since doing so would render them unusable for measuring soil respiration), we believe that a barrier in the top 1-2 cm of soil should have minimal impact on the ability of fine roots to infiltrate the soil.

Incubations were conducted by placing chamber tops, colored white to minimize solar heating, on the anchors and holding them in place with two 4.5 kg weights. Total chamber volume, installed, was approximately 5.4 L. Anchor height above the soil surface was remeasured prior to each gas sampling for each chamber to account for anchor settling and organic horizon accumulation over decadal time scales, and chamber volumes recalculated accordingly. Caps were left in place for 15 minutes, with gas samples taken via syringes at 0, 5, 10 and 15 minutes. Gas samples were withdrawn from the headspace via a stainless steel luer-lock needle that extended 2.5 cm into the headspace. Gas samples were analyzed for CO_2 concentration using a Li-Cor Li-6262 (1991-2013) or Li-7000 (2014-2016) infrared gas analyzer. Each set of syringes had associated soil temperature measurements taken at 0 and 15 minutes at a depth of 5 cm immediately adjacent to the anchor.

Soil respiration rates were calculated based on the increase in headspace CO_2 concentration over the 15 minute incubation. These data were used to parameterize exponential models relating soil CO_2 emissions to soil temperature ($\text{respiration} = \alpha e^{\beta * \text{temperature}}$). For every year the experiment was active, we parameterized a set of three models: one for the control plots, one for the heated plots while active, and one for the heated plots while inactive (i.e. when the

temperature elevation relative to the control plots was <4ºC). Each of these models drew upon all CO_2 flux rate data matching their plot and temperature designations from the year being modeled as well as from the previous year. These models were applied to the hourly soil temperature records to estimate hourly soil CO_2 emissions for each plot.

Root Respiration, Fine Root Biomass, and Soil Respiration Partitioning

Specific respiration rates for fine roots <1 mm in diameter (nmol CO_2 g^{-1} s^{-1}) were measured monthly from June through November in 2009. Roots were cut from the top 10 cm of soil, brushed free of soil, and immediately placed in a respiration cuvette where respiration rates were measured using an infrared gas analyzer (*9*). Chronic warming did not appear to affect temperature-specific fine root respiration at this site, so a single exponential model relating fine root respiration per g root biomass to soil temperature was constructed and used for both treatments (respiration = $\alpha e^{\beta * \text{temperature}}$).

Fine root biomass in the organic and mineral soil horizons (the top 10 cm of soil) was measured in 2014. Soil cores were sampled with a tulip bulb corer 5.5 cm in diameter and 10 cm deep. Soil cores were stored at 4ºC, and all processing was completed within three months of collection. Organic and mineral horizons were separated. Fine roots were picked from the soil by hand with forceps and stored in Ziploc bags on moistened paper towels at 4ºC until further processing. The remaining soil was weighed, dried at 105ºC for at least 48 hours, and reweighed to determine dry weight and moisture content. Under a dissecting microscope in a small dish of water, roots were cleaned of soil particles with paintbrushes. Roots were classified as live or dead by color, strength, and integrity of the cortex. Live and dead roots were sorted into size classes based on diameter (<1 mm, 1-4 mm, >4 mm). After cleaning and sorting, roots were dried at 60ºC for at least 48 hours and weighed. Fine root biomass was scaled from mg_{root} g_{soil}^{-1} to g_{root} m^{-2} based on previously established bulk density estimates (*9*).

For each year, the root respiration model described above was applied to this fine root biomass estimate and the hourly temperature record to calculate annual root respiration. Annual heterotrophic soil respiration was determined by subtracting annual root respiration from annual total CO_2 respiration. Annual soil carbon loss was calculated as the difference in heterotrophic respiration between the heated plots and the control plots.

Soil Carbon Stock Sampling

In 2011, soils were sampled for total organic C in the organic and mineral soil horizons. Organic horizon samples were collected in each treatment plot by removing a 20 x 20 cm square of the organic horizon layer to the depth of the mineral soil. Mineral soil samples were then collected in the same location in 10 cm increments to a depth of 30 cm using a gas-powered soil auger with a 9 cm diameter core. Samples were sieved (<2 mm) and roots, rocks and other debris >2 mm were removed. Samples were homogenized, air-dried, and a subsample (~10 g) was finely ground and analyzed for total C by dry combustion on a Costech 4010 CHNS-O Analytical Combustion System. Bulk density, determined for each sample, was used to calculate volumetric soil C stocks (g C m^{-2}).

Microbial Biomass Estimation by Direct Chloroform Extraction

In June 2016, soils were collected from the study plots and composited by treatment (disturbance control and heated) and soil horizon (organic and mineral). Microbial biomass was estimated as microbial nitrogen (N) following direct extraction with chloroform (*34*). Ten 5 g subsamples from each treatment × horizon composite sample received 20 mL of 0.5 M potassium sulfate, and 0.5 mL of ethanol-free chloroform were added to five of the subsamples. After shaking for 1 hour, chloroform was vented under a fume hood overnight. Total N was measured on a Lachat Instruments QuikChem® 8500 Series Flow Injection Analysis System following alkaline persulfate oxidation. Microbial N was calculated as the difference in N between chloroform and non-chloroform extracts divided by an extraction efficiency of 0.54.

Statistical Analysis

To determine if there was a statistically significant effect of warming on annual CO_2 fluxes for each year, the annual CO_2 fluxes from the heated plots (n = 6) and the control plots (n = 6) were compared with two-sample t-tests. Welch's correction for unequal variance was employed when necessary. For years when the data were strongly non-normally distributed (Shapiro test $P < 0.01$), Wilcoxon signed-rank tests were used instead. Statistics were run in R 3.3.2.

Delineation of Phase Boundaries

We conceptualize the transitions between phases to be a gradual process, such that there is no sharp line between them in reality. We found it beneficial for the sake of communication to delineate canonical phase boundaries. These were determined by a combination of statistical and qualitative criteria. For example, we identified Phase II as being the continuous period of time spanning years 11-17 when annual soil respiration in the heated plots was not significantly greater than the control plots.

Trends in soil respiration vs. trends in climate parameters.

To explore possible relationships between trends in soil respiration and multi-year climatic variance, we compared the warming effect on soil respiration (ΔH-C) with the mean annual temperature (MAT) and total annual precipitation (TAP) anomalies for each year visually and using linear models. Climatic data was sourced from the Shaler Meterological Station at Harvard Forest (*34*) from 1991 through 2002, and from the Fisher Meterological Station at Harvard Forest (*35*) from 2003 through 2016. MAT and TAP anomalies for each year were the difference between the year's value and the 26 year mean. We found no significant relationship between Δ(H-C)~$MAT_{anomoly}$ (P = 0.44, r^2 = -0.018), Δ(H-C)~$TAP_{anomoly}$ (P = 0.067, r^2 = 0.11), or in an ANOVA relating Δ(H-C)~$MAT_{anomaly}$ x $TAP_{anomoly}$ (MAT P = 0.426, TAP P = 0.095, MAT*TAP P = 0.537).

Winter warming

As was noted in the main text, soil warming occurs throughout the year – delta 5^{o}C – and we constantly monitor soil temperature in the control and heated plots. We used our modeled relationship between soil temperature and CO_2 flux to estimate CO_2 emissions rates throughout the year, including the winter period (1 December - 31 March). With this approach, we estimate that respiration in winter accounted for an average of 11% of total annual respiration in the control plots and 15% in the heated plots. Our over-winter estimates compare well with measurements made on a set of small plots (control and heated) adjacent to this study (*35*). The small-plot study, which was begun in 2006, uses the same heating technology and the same static-chamber gas-measurement approach. In that study, over a two-year period (2007-2008 and

2008-2009) winter warming (December-March) accounted for between 10 and 14 percent of the annual total.

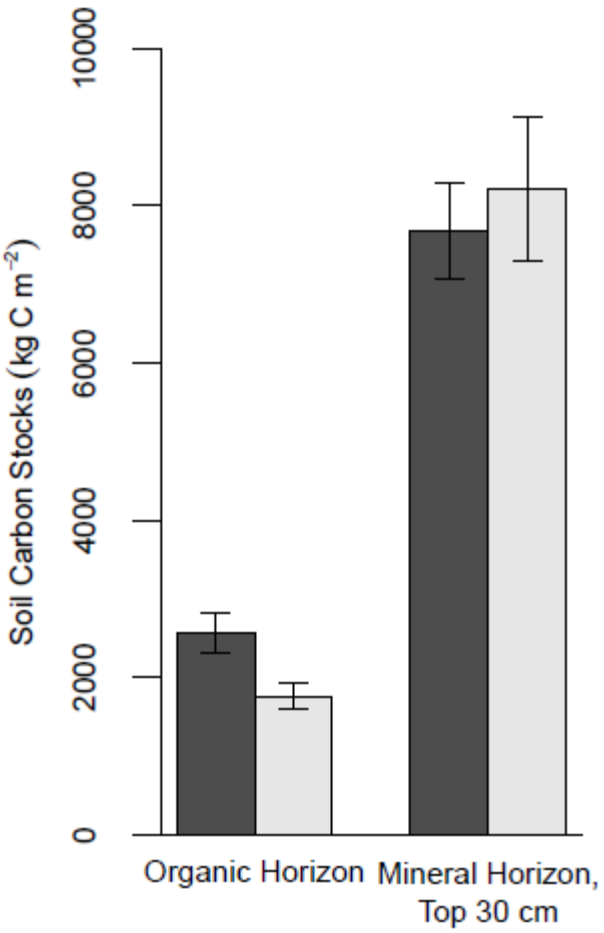

Fig. S1.

Soil carbon stocks measured in 2011. Dark grey bars represent control plots (n=6), light grey bars represent heated plots (n=6). Mineral bars represent stocks in the top 30 cm of mineral soil. Error bars represent standard error of the mean.

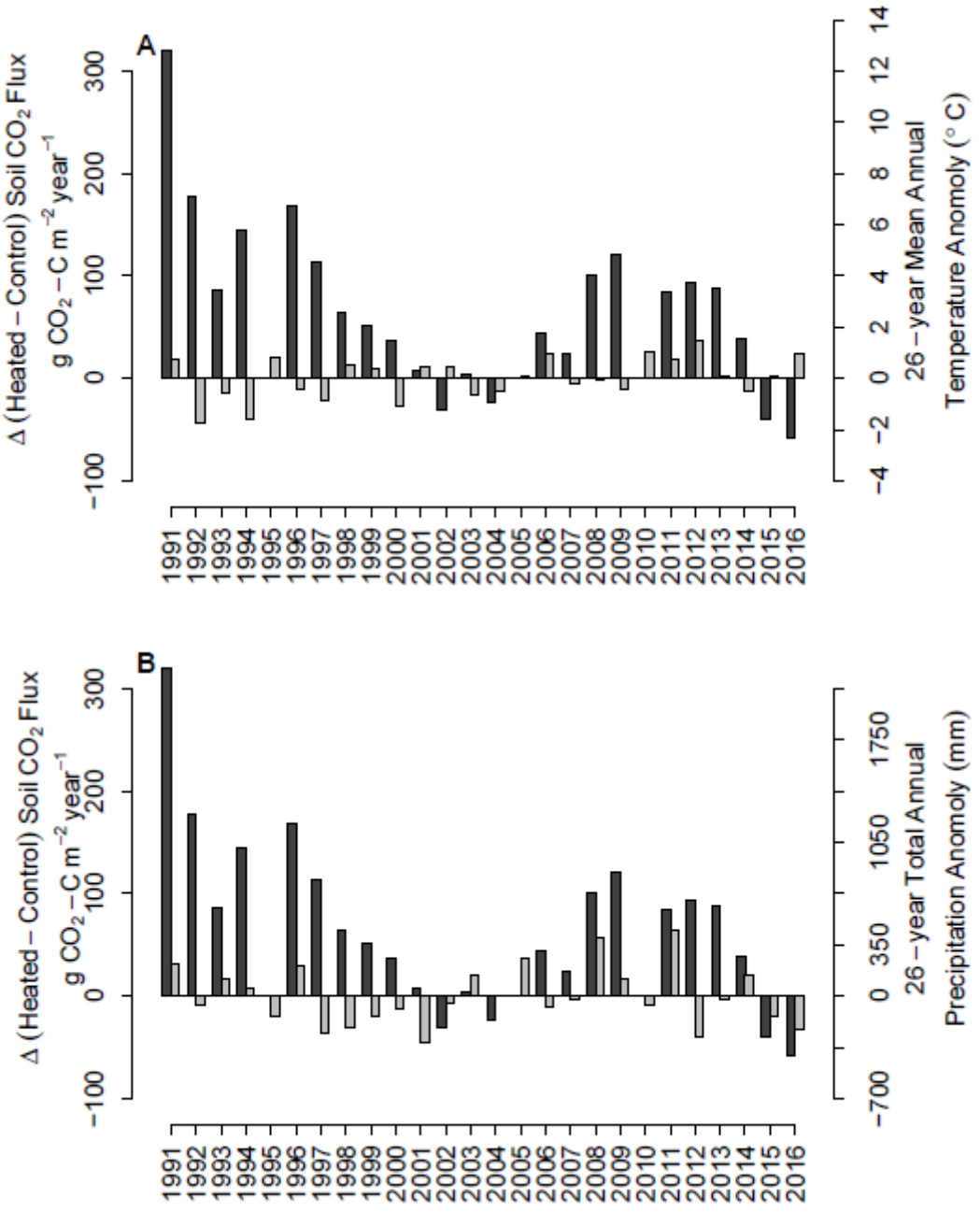

Fig. S2

Comparison of the warming effect on soil respiration (Δ[Heated-Control] annual soil respiration) to climatic variation over the 26 year span of the soil warming experiment, excluding years when the warming system was inactive for the majority of the growing season (1995, 2005, and 2010). Mean Annual Temperature (MAT) (A) and Total Annual Precipitation (TAP) (B) anomalies were calculated as the difference between the 26-year mean and the

annual value. Climatic data was sourced from the Shaler Meteorological Station at Harvard Forest (*31*) from 1991 through 2002, and from the Fisher Meteorological Station at Harvard Forest (*32*) from 2003 through 2016.

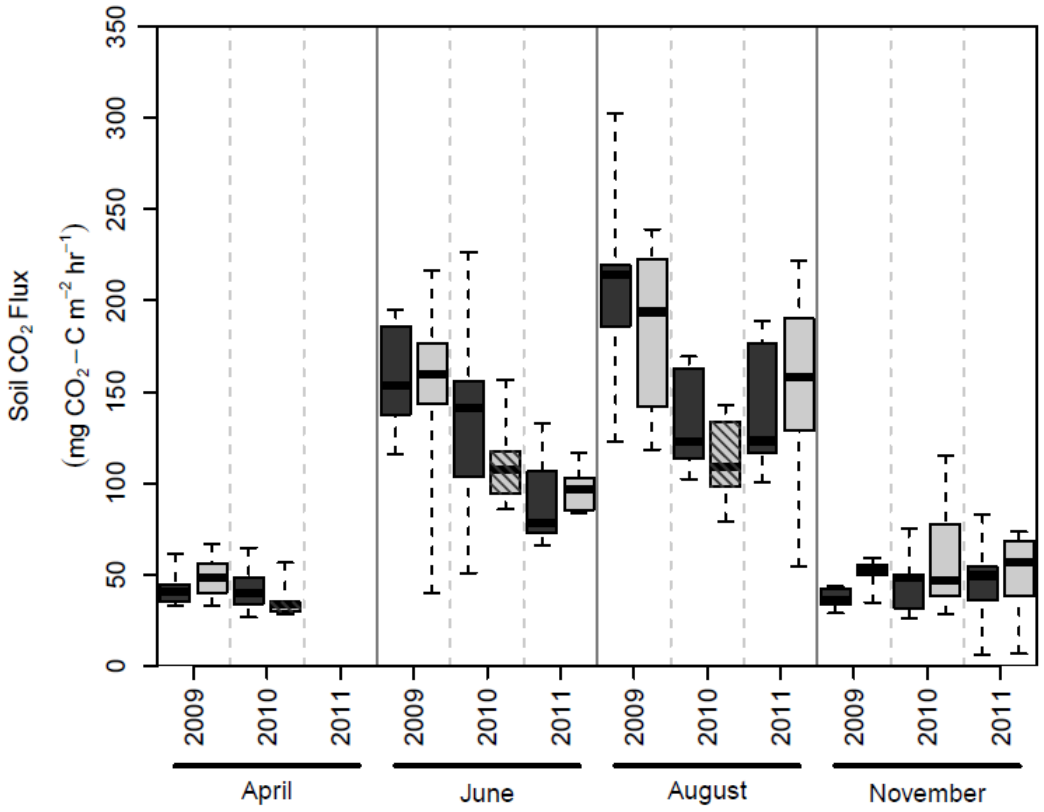

Fig. S3

Soil respiration data from 2010, when the warming system was inactive for one year, compared to soil respiration data from the previous and following years when the warming system was active, illustrating the effects of long-term acclimation of soil respiration in the heated plots relative to the control plots. Soil respiration was measured every other month in 2010; only comparable data from 2009 and 2011 is shown. Dark grey boxes represent control plots, light grey boxes represent active heated plots, light grey boxes with dark hatching represent heated plots that were inactive (no longer being heated) for at least four months prior to the time of sampling. For each box (n=6), the thick black bar represents the median value, the rectangle represents the interquartile range, and the whiskers extend to the most extreme points.

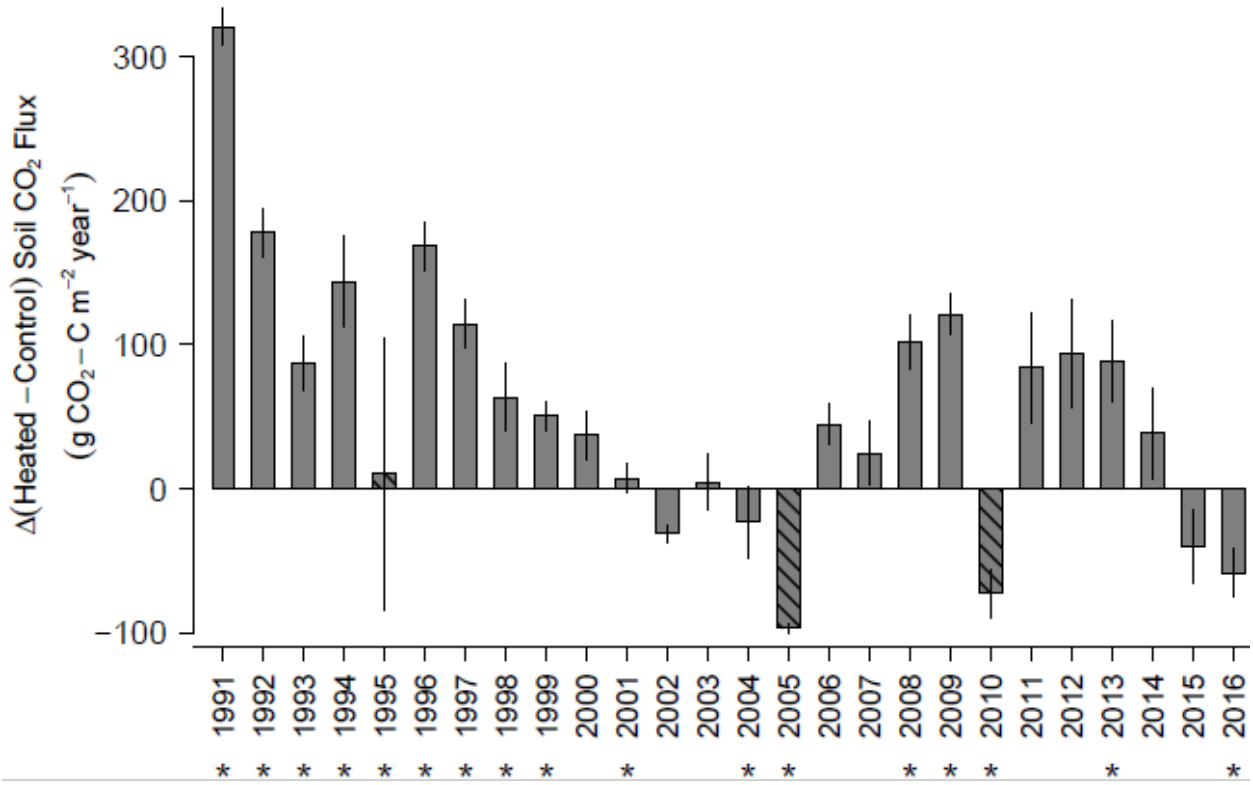

Fig S4

Annual increase in soil CO_2 emissions in the heated plots relative to the control plots. Hatched bars represent years when the heating system was inactive for the majority of the growing season. Error bars represent standard error of the mean, derived from the standard error estimates in Fig 1A and propagated through the operations necessary to produce this figure (n=6,6). Asterisks denote years when the heated and control plots were significantly different (paired-sample t-tests or Wilcoxon signed-rank tests as appropriate, n=(6,6), *P < 0.05; see Statistical Analysis section).

References

1. J. G. Canadell, C. Le Quéré, M. R. Raupach, C. B. Field, E. T. Buitenhuis, P. Ciais, T. J. Conway, N. P. Gillett, R. A. Houghton, G. Marland, Contributions to accelerating atmospheric CO_2 growth from economic activity, carbon intensity, and efficiency of natural sinks. *Proc. Natl. Acad. Sci. U.S.A.* **104**, 18866–18870 (2007). doi:10.1073/pnas.0702737104 Medline

2. P. Friedlingstein, P. Cox, R. Betts, L. Bopp, W. von Bloh, V. Brovkin, P. Cadule, S. Doney, M. Eby, I. Fung, G. Bala, J. John, C. Jones, F. Joos, T. Kato, M. Kawamiya, W. Knorr, K. Lindsay, H. D. Matthews, T. Raddatz, P. Rayner, C. Reick, E. Roeckner, K.-G. Schnitzler, R. Schnur, K. Strassmann, A. J. Weaver, C. Yoshikawa, N. Zeng, Climate-carbon cycle feedback analysis: Results from the C4MIP model intercomparison. *J. Clim.* **19**, 3337–3353 (2006). doi:10.1175/JCLI3800.1

3. M. Heimann, M. Reichstein, Terrestrial ecosystem carbon dynamics and climate feedbacks. *Nature* **451**, 289–292 (2008). doi:10.1038/nature06591 Medline

4. P. Ciais *et al*., Carbon and other biogeochemical cycles. In *Climate Change 2013: The Physical Science Basis. Working Group I Contribution to the IPCC Fifth Assessment Report (AR5)* (IPCC, Geneva, 2013).

5. E. A. Davidson, I. A. Janssens, Temperature sensitivity of soil carbon decomposition and feedbacks to climate change. *Nature* **440**, 165–173 (2006). doi:10.1038/nature04514 Medline

6. M. W. I. Schmidt, M. S. Torn, S. Abiven, T. Dittmar, G. Guggenberger, I. A. Janssens, M. Kleber, I. Kögel-Knabner, J. Lehmann, D. A. C. Manning, P. Nannipieri, D. P. Rasse, S. Weiner, S. E. Trumbore, Persistence of soil organic matter as an ecosystem property. *Nature* **478**, 49–56 (2011). doi:10.1038/nature10386 Medline

7. M. Lu, X. Zhou, Q. Yang, H. Li, Y. Luo, C. Fang, J. Chen, X. Yang, B. Li, Responses of ecosystem carbon cycle to experimental warming: A meta-analysis. *Ecology* **94**, 726–738 (2013). doi:10.1890/12-0279.1 Medline

8. J. M. Melillo, D. W. Kicklighter, A. D. McGuire, W. T. Peterjohn, K. M. Newkirk, Global change and its effects on soil carbon stocks. In *The Role of Nonliving Organic Matter in the Earth's Carbon Cycle*, R. Zepp, C. Sonntag, Eds. (Wiley, 1995), pp. 175–189.

9. J. M. Melillo, P. A. Steudler, J. D. Aber, K. Newkirk, H. Lux, F. P. Bowles, C. Catricala, A. Magill, T. Ahrens, S. Morrisseau, Soil warming and carbon-cycle feedbacks to the climate system. *Science* **298**, 2173–2176 (2002). doi:10.1126/science.1074153 Medline

10. J. M. Melillo, S. Butler, J. Johnson, J. Mohan, P. Steudler, H. Lux, E. Burrows, F. Bowles, R. Smith, L. Scott, C. Vario, T. Hill, A. Burton, Y.-M. Zhou, J. Tang, Soil warming, carbon-

nitrogen interactions, and forest carbon budgets. *Proc. Natl. Acad. Sci. U.S.A.* **108**, 9508–9512 (2011). doi:10.1073/pnas.1018189108 Medline

11. A. P. Sokolov, D. W. Kicklighter, J. M. Melillo, B. S. Felzer, C. A. Schlosser, T. W. Cronin, Consequences of considering carbon-nitrogen interactions on the feedbacks between climate and the terrestrial carbon cycle. *J. Clim.* **21**, 3776–3796 (2008). doi:10.1175/2008JCLI2038.1

12. P. E. Thornton, S. C. Doney, K. Lindsay, J. K. Moore, N. Mahowald, J. T. Randerson, I. Fung, J.-F. Lamarque, J. J. Feddema, Y.-H. Lee, Carbon-nitrogen interactions regulated climate-carbon cycle feedbacks: Results from an atmosphere-ocean general circulation model. *Biogeosciences* **6**, 2099–2120 (2009). doi:10.5194/bg-6-2099-2009

13. W. T. Peterjohn, J. M. Melillo, F. P. Bowles, P. A. Steudler, Soil warming and trace gas fluxes: Experimental design and preliminary flux results. *Oecologia* **93**, 18–24 (1993). doi:10.1007/BF00321185 Medline

14. W. T. Peterjohn, J. M. Melillo, P. A. Steudler, K. M. Newkirk, F. P. Bowles, J. D. Aber, The response of trace gas fluxes and N availability to elevated soil temperatures. *Ecol. Appl.* **4**, 617–625 (1994). doi:10.2307/1941962

15. C. E. Hicks Pries, C. Castanha, R. C. Porras, M. S. Torn, The whole-soil carbon flux in response to warming. *Science* **355**, 1420–1423 (2017). doi:10.1126/science.aal1319 Medline

16. Y. Luo, S. Wan, D. Hui, L. L. Wallace, Acclimatization of soil respiration to warming in a tall grass prairie. *Nature* **413**, 622–625 (2001). doi:10.1038/35098065 Medline

17. S. D. Frey, R. Drijber, H. Smith, J. M. Melillo, Microbial biomass, functional capacity, and community structure after 12 years of soil warming. *Soil Biol. Biochem.* **40**, 2904–2907 (2008). doi:10.1016/j.soilbio.2008.07.020

18. M. A. Bradford, C. A. Davies, S. D. Frey, T. R. Maddox, J. M. Melillo, J. E. Mohan, J. F. Reynolds, K. K. Treseder, M. D. Wallenstein, Thermal adaptation of soil microbial respiration to elevated temperature. *Ecol. Lett.* **11**, 1316–1327 (2008). doi:10.1111/j.1461-0248.2008.01251.x Medline

19. G. Pold, A. S. Grandy, J. M. Melillo, K. M. DeAngelis, Changes in substrate availability drive carbon cycle response to chronic warming. *Soil Biol. Biochem.* **110**, 68–78 (2017). doi:10.1016/j.soilbio.2017.03.002

20. K. M. DeAngelis, G. Pold, B. D. Topçuoğlu, L. T. van Diepen, R. M. Varney, J. L. Blanchard, J. Melillo, S. D. Frey, Long-term forest soil warming alters microbial communities in temperate forest soils. *Front. Microbiol.* **6**, 104 (2015). doi:10.3389/fmicb.2015.00104 Medline

21. G. Pold, J. M. Melillo, K. M. DeAngelis, Two decades of warming increases diversity of a potentially lignolytic bacterial community. *Front. Microbiol.* **6**, 480 (2015). doi:10.3389/fmicb.2015.00480 Medline

22. G. Pold, A. F. Billings, J. L. Blanchard, D. B. Burkhardt, S. D. Frey, J. M. Melillo, J. Schnabel, L. T. A. van Diepen, K. M. DeAngelis, Long-term warming alters carbohydrate degradation potential in temperate forest soils. *Appl. Environ. Microbiol.* **82**, 6518–6530 (2016). doi:10.1128/AEM.02012-16 Medline

23. S. D. Frey, J. Lee, J. M. Melillo, J. Six, The temperature response of microbial efficiency and its feedback to climate. *Nat. Clim. Chang.* **3**, 395–398 (2013). doi:10.1038/nclimate1796

24. S. D. Allison, M. D. Wallenstein, M. A. Bradford, Soil-carbon response to warming dependent on microbial physiology. *Nat. Geosci.* **3**, 336–340 (2010). doi:10.1038/ngeo846

25. S. E. Trumbore, Potential responses of soil organic carbon to global environmental change. *Proc. Natl. Acad. Sci. U.S.A.* **94**, 8284–8291 (1997). doi:10.1073/pnas.94.16.8284 Medline

26. T. W. Crowther, K. E. O. Todd-Brown, C. W. Rowe, W. R. Wieder, J. C. Carey, M. B. Machmuller, B. L. Snoek, S. Fang, G. Zhou, S. D. Allison, J. M. Blair, S. D. Bridgham, A. J. Burton, Y. Carrillo, P. B. Reich, J. S. Clark, A. T. Classen, F. A. Dijkstra, B. Elberling, B. A. Emmett, M. Estiarte, S. D. Frey, J. Guo, J. Harte, L. Jiang, B. R. Johnson, G. Kröel-Dulay, K. S. Larsen, H. Laudon, J. M. Lavallee, Y. Luo, M. Lupascu, L. N. Ma, S. Marhan, A. Michelsen, J. Mohan, S. Niu, E. Pendall, J. Peñuelas, L. Pfeifer-Meister, C. Poll, S. Reinsch, L. L. Reynolds, I. K. Schmidt, S. Sistla, N. W. Sokol, P. H. Templer, K. K. Treseder, J. M. Welker, M. A. Bradford, Quantifying global soil carbon losses in response to warming. *Nature* **540**, 104–108 (2016). doi:10.1038/nature20150 Medline

27. E. G. Jobbágy, R. B. Jackson, The vertical distribution of soil organic carbon and its relation to climate and vegetation. *Ecol. Appl.* **10**, 423–436 (2000). doi:10.1890/1051-0761(2000)010[0423:TVDOSO]2.0.CO;2

28. J. Rousk, P. W. Hill, D. L. Jones, Priming of the decomposition of ageing soil organicmatter: Concentration dependence and microbial control. *Funct. Ecol.* **29**, 285–296 (2015). doi:10.1111/1365-2435.12377

29. C. Le Quéré, R. M. Andrew, J. G. Canadell, S. Sitch, J. I. Korsbakken, G. P. Peters, A. C. Manning, T. A. Boden, P. P. Tans, R. A. Houghton, R. F. Keeling, S. Alin, O. D. Andrews, P. Anthoni, L. Barbero, L. Bopp, F. Chevallier, L. P. Chini, P. Ciais, K. Currie, C. Delire, S. C. Doney, P. Friedlingstein, T. Gkritzalis, I. Harris, J. Hauck, V. Haverd, M. Hoppema, K. Klein Goldewijk, A. K. Jain, E. Kato, A. Körtzinger, P. Landschützer, N. Lefèvre, A. Lenton, S. Lienert, D. Lombardozzi, J. R. Melton, N. Metzl, F. Millero, P. M.

S. Monteiro, D. R. Munro, J. E. M. S. Nabel, S. Nakaoka, K. O'Brien, A. Olsen, A. M. Omar, T. Ono, D. Pierrot, B. Poulter, C. Rödenbeck, J. Salisbury, U. Schuster, J. Schwinger, R. Séférian, I. Skjelvan, B. D. Stocker, A. J. Sutton, T. Takahashi, H. Tian, B. Tilbrook, I. T. van der Laan-Luijkx, G. R. van der Werf, N. Viovy, A. P. Walker, A. J. Wiltshire, S. Zaehle, Global carbon budget 2016. *Earth Syst. Sci. Data* **8**, 605–649 (2016). doi:10.5194/essd-8-605-2016

30. R. S. DeFries, C. B. Field, I. Fung, G. J. Collatz, L. Bounoua, Combining satellite data and biogeochemical models to estimate global effects of human-induced land cover change on carbon emissions and primary productivity. *Global Biogeochem. Cycles* **13**, 803–815 (1999). doi:10.1029/1999GB900037

31. E. Boose, E. Gould, *Shaler Meteorological Station at Harvard Forest 1964–2002* (Harvard Forest Data Archive HF000, 1999).

32. E. Boose, *Fisher Meteorological Station at Harvard Forest Since 2001* (Harvard Forest Data Archive HF001, 2001).

33. R. D. Bowden, J. M. Melillo, P. A. Steudler, J. D. Aber, Effects of nitrogen additions on annual nitrous oxide fluxes from temperate forest soils in the northeastern United States. *J. Geophys. Res.* **96**, 9321–9328 (1991). doi:10.1029/91JD00151

34. R. Setia, S. L. Verma, P. Marschner, Measuring microbial biomass carbon by direct extraction–comparison with chloroform fumigation-extraction. *Eur. J. Soil Biol.* **53**, 103–106 (2012). doi:10.1016/j.ejsobi.2012.09.005

35. A. R. Contosta, S. D. Frey, A. B. Cooper, Seasonal dynamics of soil respiration and N mineralization in chronically warmed and fertilized soils. *Ecosphere* **2**, 36 (2011). doi:10.1890/ES10-00133.1